AIAA JOURNAL
Vol. 46, No. 3, March 2008

Forebody Slot Blowing on Vortex Breakdown and Load Over a Delta Wing

Y. D. Cui,* T. T. Lim,† and H. M. Tsai‡
National University of Singapore,
Singapore 117508, Republic of Singapore

DOI: 10.2514/1.34293

Previous study (Cui, Y. D., Lim, T. T., and Tsai, H. M., "Control of Vortex Breakdown Over a Delta Wing Using Forebody Slot Blowing," *AIAA Journal*, Vol. 45, No. 1, 2007, pp. 110–117.) shows that a forebody slot blowing technique significantly delays vortex breakdown over a delta wing. Blowing only on one side while delaying vortex breakdown has an opposite effect on the nonblowing side. Although the authors provided a plausible explanation for the observed behavior, no concrete evidence was given. In this paper, we address this issue and further evaluate the effects of symmetric and differential blowing on the aerodynamic loads. Flow visualization and force measurement were carried out in a water tunnel at a Reynolds number of 8.5×10^4. Our study shows that the differing effect of differential blowing can be traced to a combination of forebody slot blowing itself and the interaction of the vortices from both sides resulting in a side-slip-like effect. Moreover, symmetrical forebody slot blowing, apart from producing a significant delay in the formation of vortex breakdown, increases the lift by more than 5%. Differential blowing can be used to manipulate the vortex breakdown position and change the roll moment of the wing, which suggests that the method can be a potential means for roll control.

Nomenclature

A_j	=	slot area
C_L	=	lift coefficient, lift$/(qS)$
C_l	=	roll moment coefficient, roll moment$/(qSc)$
C_μ	=	blowing momentum coefficient, $\rho Q^2/(A_j q S)$
$C_{\mu P}$	=	blowing momentum coefficient for port side slot
$C_{\mu S}$	=	blowing momentum coefficient for starboard side slot
c	=	root chord
Q	=	volume flow rate of blowing
q	=	dynamic pressure of freestream
Re	=	Reynolds number, Uc/v
S	=	area of delta wing
U	=	freestream velocity
V_j	=	average slot exit velocity
X_b	=	vortex breakdown position from the apex of the wing
$X_{b\text{mean}}$	=	mean vortex breakdown position
$(X_{b\text{mean}})_P$	=	mean port side vortex breakdown position
$(X_{b\text{mean}})_S$	=	mean starboard side vortex breakdown position
v	=	kinematic viscosity of water
ρ	=	density of blowing fluid

I. Introduction

IT IS known that vortex breakdown over a delta wing, first reported by Peckham and Atkinson in 1957 [1] has detrimental effects on not only the aerodynamic characteristics of the wing, such as a reduction in lift, an increase in drag, and changes in moment characteristics, but also heightened structural fatigue due to strong pressure fluctuations, unsteadiness, and vibrations. The overall aircraft's performance, controllability, and maneuverability can be severely affected. Over the decades, much effort has been attempted to understand the physics of this flow phenomenon [2–7].

On the other hand, the need to control vortex breakdown over a delta wing at high angles of attack has motivated many researchers to propose various flow control techniques (see the review article by Mitchell and Délery [8]). These include mechanical devices such as leading-edge flaps [9–12], apex fences [13], canards, strakes, leading-edge extensions (LEXs), or double-delta wing [14–22] and pneumatic techniques such as trailing-edge blowing [23–28] or suction [29], along-the-core blowing technique [30–34], spanwise blowing (SWB) [35–37], and some other blowing/suction techniques [38] with different blowing/suction locations and orientations.

It is generally believed that trailing-edge blowing [23–28] or suction [29] techniques delay vortex breakdown by decreasing the downstream pressure gradient, and along-the-core blowing technique [30–34] delays vortex breakdown by increasing the axial velocity (i.e., a reduction in the swirl number). Dixon [35] believed that SWB on the wing provides sweeplike effects as the SWB jets are entrained in the leading-edge vortices. Bradley and Wray [38] credited the success of their blowing technique to the increase in the vortex stability, which to some extent is related to the longitudinal flow in the vortex core. Passive vortex breakdown control devices such as strakes, LEXs, or double-delta wings [14–22] are used in numerous aircrafts. They modify the flowfield by inducing a nonuniform distribution of local angles of attack at the wing, leading to the generation of a nonconical vortex formation and a corresponding delay in vortex breakdown over the wing [16,18,21].

In our previous study [39], we proposed a control method which is referred to as forebody slot blowing that exploits the benefits of both the spanwise slot blowing and the effectiveness of canards. Flow visualizations show that this technique can be used to delay vortex breakdown on a delta wing more effectively than some existing blowing techniques. However, due to the constraints of the experimental setup, the study did not resolve the issue of why a single side blowing delays the formation of vortex breakdown on the blowing side but has an opposite effect on the nonblowing side. In this paper, we attempt to address this issue by systematically

Part of the work has been presented as Paper AIAA-2007-0882 at the 45th AIAA Aerospace Sciences Meeting and Exhibit, Reno, Nevada, 8–11 January 2007; received 28 August 2007; revision received 28 October 2007; accepted for publication 11 November 2007.

*Associate Scientist, Temasek Laboratories, 5 Sports Drive 2. Member AIAA.

†Professor, Department of Mechanical Engineering, 9 Engineering Drive 1, Singapore 117576.

‡Senior Research Scientist, Temasek Laboratories, 5 Sports Drive 2. Member AIAA.

isolating the possible causes. To this end, a delta wing-body configuration model that effectively incorporates two separate compartments for blowing was fabricated. This model also enables us to carry out force measurement and to evaluate the aerodynamic effects of symmetrical and differential forebody slot blowing.

II. Experimental Details

The experiments were conducted in the water tunnel located in Temasek Laboratories of the National University of Singapore. The test section of the water tunnel measures 1.0 m high (height of the water surface), 0.75 m wide, and 2.25 m long. It is surrounded by tempered glass on the two sides and at the bottom, which allows high-quality flow visualization from almost any angle. Although the water tunnel can achieve a maximum velocity of 0.9 m/s in the test section, the speed selected for the present study was about 0.29 m/s with the corresponding turbulence intensity of about 1%. Figure 1 shows the schematic drawing of the experimental setup in the water tunnel. A level supporting platform was constructed over the test section for a reference plane. A rotation gauge with resolution of 1/60 deg was mounted to this platform to adjust accurately the side-slip angle. A force balance was then mounted on this rotation gauge on one end and connected to an angle mechanism on the other end, which in turn was connected to a streamlined strut. The angle of attack (AOA) was set by predetermined pin holes on an inclined angle mechanism with the accuracy of about 0.5 deg. The force balance has an accuracy of about ±0.10 N for the lift measurement, which corresponds to an error of about ±3% for the maximum lift coefficient at the operating water tunnel speed. No side slip or roll angle was considered in the present investigation; therefore, these angles were carefully set to zero to ensure flow symmetry. The experimental model was set upside down to avoid interferences from the free surface and for ease of capturing flow images.

A delta wing-body configuration model was used in the experiment (see Fig. 2). This model has a sweep angle of 60 deg, root chord length of 300 mm, thickness of 5 mm, and was fabricated from a marine-grade aluminum plate. The leading edges of the wing are beveled at 45 deg on the windward sides. To afford differential forebody slot blowing and to ensure the uniformity of the slot exit velocity, a relatively large forebody was used in this study, though additional drag can be caused by this. The forebody was fabricated from a cylindrical brass bar of 24 mm outside diameter (D) with a tangent ogive tip with a fineness ratio of 1.5. The ogive tip was located 6.25D upstream of the apex of the wing. Additional tests show that tip vortices from the forebody had minimal influence on the flowfield around the wing. Two separated hollow cavities inside the forebody served as chambers from which the blowing fluid can be separately ejected to realize differential blowing. Each chamber was connected to a flexible tube via a copper tube inside the model (see Fig. 2). These flexible tubes were connected to a piping system including a pump, a ball valve for flow rate control, and a flowmeter for flow rate measurement. They were also used to allow free

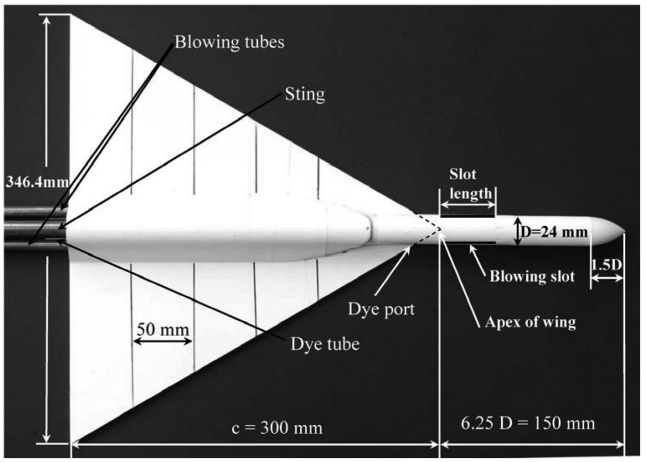

Fig. 2 Generic delta wing-body model with a 60-deg sweep angle.

movement to reduce the coupling forces between the jet feed system and the model. The blowing slots with a rectangular shape were machined at the center plane of the forebody cylinder and parallel to the wing. Each slot has a predetermined length of 40 mm and width of 0.5 mm, and the end of the slot is located at the apex of the wing. Four reference lines parallel to the trailing edge were marked on the delta wing for the purpose of identifying vortex breakdown position. At a high angle of attack of 30 deg, the blockage ratio of the model in the water tunnel is about 3.5% and as such the blockage effect of the model is insignificant for the purposes of the present study.

To visualize the flow, a mixture of food dye and water (diluted with alcohol to achieve the specific gravity of approximately 1) was released slowly through the dye ports embedded in the model. The flow rate of the dye was regulated via miniature valves to minimize flow interference. In all cases, flow images were captured by a charge-coupled device (CCD) video camera for subsequently analysis.

The Reynolds number based on root chord length and the freestream velocity (about 29 cm/s) was about 8.5×10^4. The flow was studied at angles of attack of 17, 22, 26, 28, and 30 deg. The effect of slot blowing is quantified by a common parameter called blowing momentum coefficient, which is defined as $C_\mu = \rho Q^2/(A_j q S)$, where ρ is the density of the blowing fluid, Q is the volume flow rate through slot(s), A_j is the slot area, q is the dynamic pressure of the freestream, and S is the area of the delta wing. Assuming the slot velocity is uniform, the corresponding slot velocity ratio (V_j/U) can also be obtained by using this momentum coefficient, that is, $V_j/U = 0.5 C_\mu US/Q$, where U is the freestream velocity. For completeness, Fig. 3 provides the slot velocity ratio variation with C_μ for one blowing slot at the parameters used in this study, though the slot velocity ratio is not used as a control parameter in the following sections.

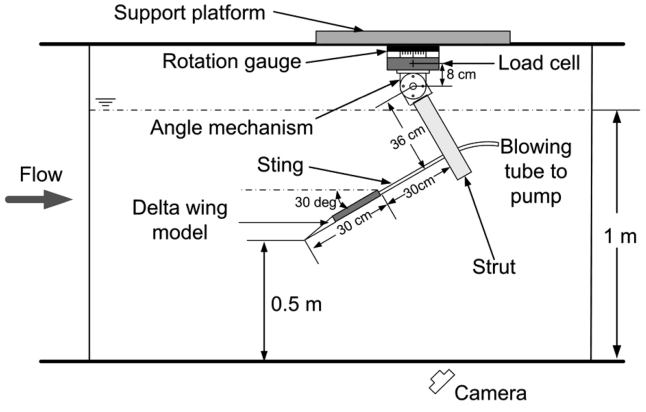

Fig. 1 Schematic of the experimental setup used.

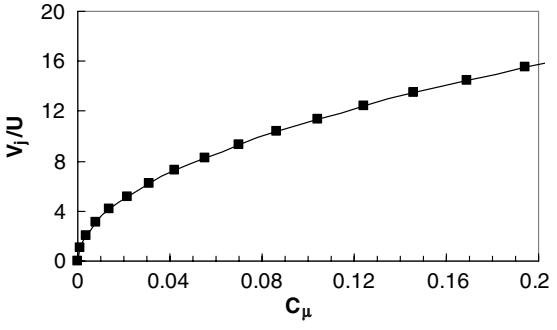

Fig. 3 Relationship between C_μ and slot velocity ratio V_j/U for one slot at the parameters used in this study.

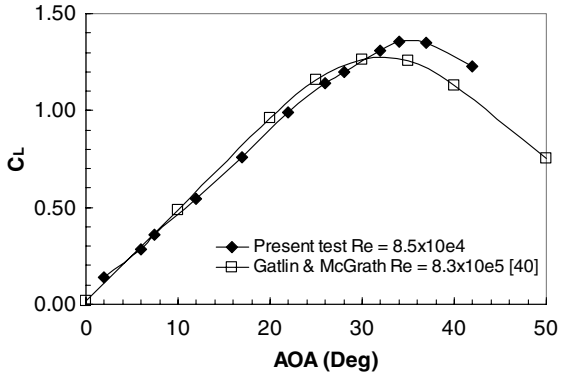

Fig. 4 Comparison of the measured lift coefficient with published data for a 65-deg delta wing to verify the accuracy of the force balance.

III. Results and Discussions

Changes in the vortex breakdown location and normal force are used to evaluate the effects of forebody slot blowing. Because the model used in the present experiment is different from the one in our previous study, some flow visualization was carried out to check for repeatability with the earlier results. As in the previous study [39], time-averaged images were used to determine the mean breakdown location with uncertainty of less than 2%.

To assess the force measurement system, a preliminary test was carried out for a plain 65-deg delta wing model. This delta wing has a sweep angle of 65 deg, root chord length of 300 mm, thickness of 6 mm, with the leading edges of the wing beveled at 45 deg on the windward sides. Figure 4 shows the present measured lift coefficients together with the available published lift coefficient data [40] which was made at 10 times higher Reynolds number. As to be expected of sharp-edged delta wings, the results indicate that the lift coefficient is insensitive to Reynolds numbers when it is below the maximum value. Previously, Munro et al. [41] also reported force measurements over a 65-deg delta wing in a water tunnel, but only normal force rather than lift coefficients are presented and hence could not be included for direct comparison. It is seen in Fig. 4 that the present results are in good general agreement with the published data [40], thus indicating that our force measurement system is suitable for the present study to evaluate the aerodynamic behavior of the control devices. Small differences at higher angles of attack can be attributed to minor differences in the model/sting and the experimental conditions used in the other measurements.

Before presenting the force measurements, it is worthwhile to note how the measurements were made. The effects of the sting and the strut on the force measurement are not taken in consideration because the force contributed by them (without the delta wing) is comparatively small so that it is outside the working range of the force balance. Nevertheless, to minimize the error measured by the force balance due to uncertainties, the following strategy was adopted. At any given angles of attack, the normal force from the balance without blowing was first obtained and was repeated twice to obtain an average value. The force balance system was then zeroed and the changes in the normal force due to blowing were taken when the blowing was applied. This process was repeated several times to obtain the averaged value. It should be noted that the blowing itself has some effects on the force measurement. It was found that the blowing produced a small negative normal force at the condition of "pure blowing," where the water tunnel speed was zero. For the force data presented here, the effect of pure blowing was not taken into account because the small magnitude of the force is outside the working range of the force balance. Thus, the presented data are relatively conservative. For the study involving differential blowing, because the blowing plane was not the same as the force balance reference plane, it would therefore produce an additional roll moment. Hence, for the roll moment data presented here, the effect of differential blowing was taken into account by subtracting the additional roll moment due to pure differential blowing only.

A. Symmetrical Blowing

Figures 5 and 6 present typical time-averaged flow images for symmetrical blowing at the angles of attack of 17 and 28 deg and $Re = 8.5 \times 10^4$. The overall effects of symmetry blowing on vortex breakdown locations are summarized in Fig. 7, which are consistent with our previous study [39] where the vortex breakdown location increases with increasing blowing momentum coefficient C_μ. With increasing angles of attack, larger blowing momentum is necessary

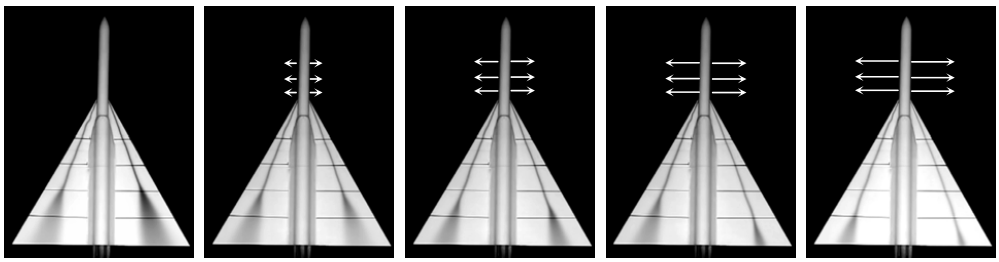

a) C_μ= 0.0 **b) C_μ= 0.016** **c) C_μ= 0.028** **d) C_μ = 0.042** **e) C_μ = 0.062**

Fig. 5 Time-averaged images of vortex breakdown structures for different blowing momentum coefficient C_μ for symmetric blowing at AOA = 17 deg. Arrows indicate the direction of forebody slot blowing.

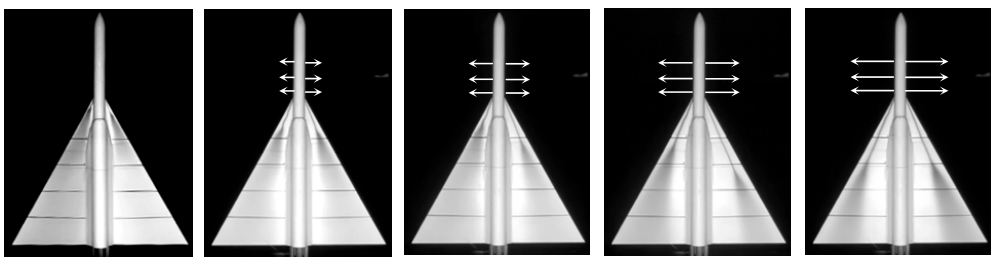

a) C_μ= 0.0 **b) C_μ= 0.028** **c) C_μ= 0.062** **d) C_μ = 0.559** **e) C_μ = 1.162**

Fig. 6 Time-averaged images of vortex breakdown structures for different blowing momentum coefficient C_μ for symmetric blowing at AOA = 28 deg. Arrows indicate the direction of forebody slot blowing.

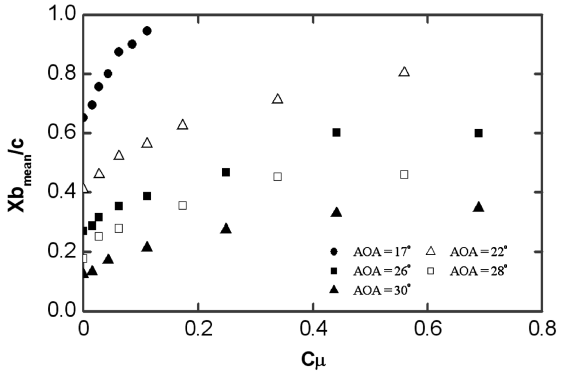

Fig. 7 Vortex breakdown location versus blowing momentum coefficient C_μ for various angles of attack.

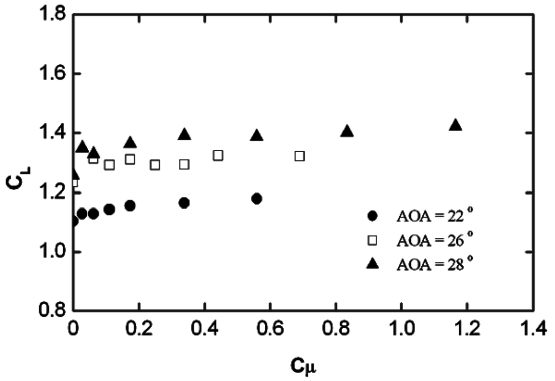

Fig. 8 Measured lift coefficient versus blowing momentum coefficient C_μ for three angles of attack.

to increase the vortex breakdown location. Asymmetric breakdown can occur as the blowing momentum coefficients are increased even at the condition of symmetric blowing. This is likely due to a slight alignment error in the apparatus as well as the interaction of the two main separated vortices.

Figure 8 shows the effects of blowing on the lift coefficient at three different angles of attack demonstrating the expected increase in lift when vortex breakdown is delayed. The selected angles are those where vortex breakdown is obvious and demonstrative. It can be seen from the figure that although the lift coefficient increased with the blowing momentum coefficient C_μ, the rate of increase is higher at low blowing momentum and attained a maximum value of about 5% at $C_\mu = 0.2$. Above $C_\mu = 0.2$, there is no significant increase in C_L. This result is consistent with the flow visualizations which show that low blowing momentum coefficients are sufficiently effective in delaying the initiation of vortex breakdown. At low values of momentum coefficient C_μ, the measured data appear to be scattered. This could be attributed to the sensitivity of the vortex breakdown location on the blowing rate, and a small variation of the blowing rate may cause a large fluctuation on the vortex breakdown position.

B. Differential Blowing

Figure 9 presents the flow visualization results at AOA $= 22$ deg with differential blowing. It is observed that with only the port side blowing, the port side vortex breakdown position is delayed, but the starboard side vortex breakdown position is promoted forward toward the apex. For example, in Fig. 9d when $C_{\mu P} = 0.086$ and $C_{\mu S} = 0.0$, it can be seen that the port side vortex breakdown position is significantly delayed beyond the root of the wing, while the starboard side vortex breakdown position is promoted toward the wing apex. While keeping $C_{\mu P} = 0.086$, increasing $C_{\mu S}$ to 0.022 leads to a delay in the breakdown position at the starboard side and the promotion of vortex breakdown position at the port side (see Fig. 9e). Similar results were obtained for AOA $= 28$ deg (see Fig. 10). These results clearly show that the forebody slot blowing has favorable effect on the blowing side and unfavorable effect on the opposite side.

The above flow visualization results clearly indicate that differential blowing leads to asymmetric vortex breakdown, which will undoubtedly affect the roll moment. This is evident from the roll moment measurements presented in Fig. 11 for differential blowing for AOA $= 22$ deg and 28 deg. It can be seen from the figure that with the port side blowing, the overall roll moment increased with the port side blowing momentum $C_{\mu P}$. This is consistent with the flow visualization results which show that the port side blowing delays

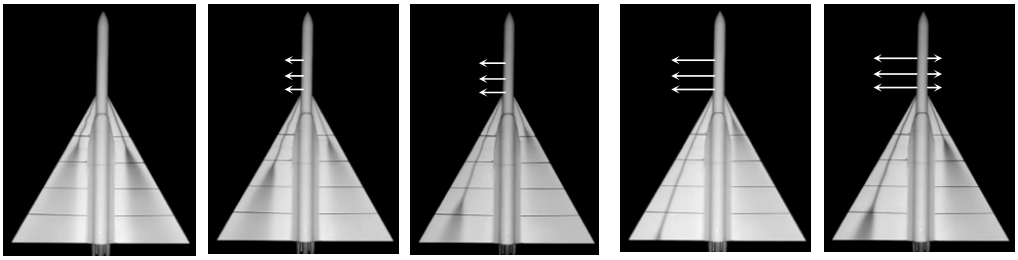

a) $C_{\mu P} = 0.0$, $C_{\mu S} = 0.0$ **b) $C_{\mu P} = 0.031$, $C_{\mu S} = 0.0$** **c) $C_{\mu P} = 0.055$, $C_{\mu S} = 0.0$** **d) $C_{\mu P} = 0.086$, $C_{\mu S} = 0.0$** **e) $C_{\mu P} = 0.086$, $C_{\mu S} = 0.022$**

Fig. 9 Time-averaged images of vortex breakdown structures for differential blowing at AOA $= 22$ deg.

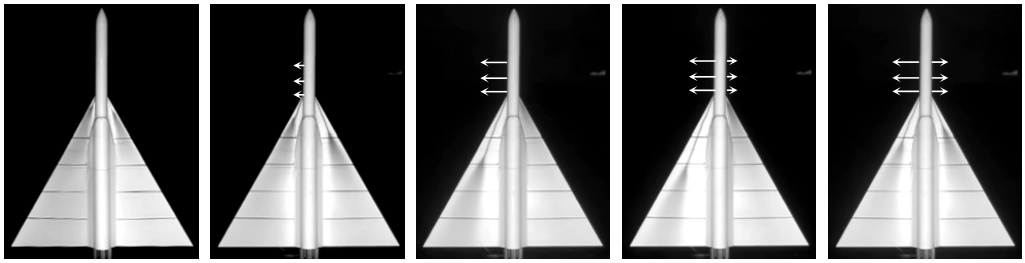

a) $C_{\mu P} = 0.0$, $C_{\mu S} = 0.0$ **b) $C_{\mu P} = 0.014$, $C_{\mu S} = 0.0$** **c) $C_{\mu P} = 0.055$, $C_{\mu S} = 0.0$** **d) $C_{\mu P} = 0.055$, $C_{\mu S} = 0.014$** **e) $C_{\mu P} = 0.055$, $C_{\mu S} = 0.031$**

Fig. 10 Time-averaged images of vortex breakdown structures for differential blowing at AOA $= 28$ deg.

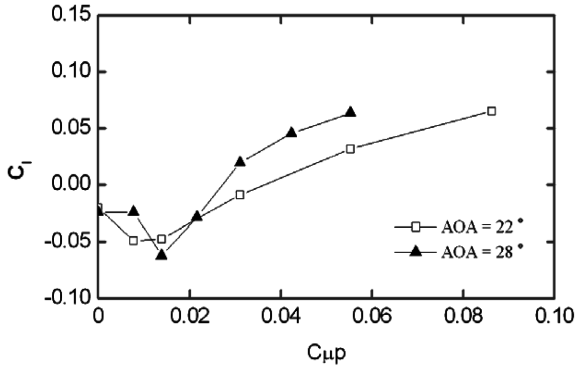

Fig. 11 Roll moment coefficient C_l with $C_{\mu P}$ for port side blowing only ($C_{\mu S} = 0$) at AOA = 22 deg and 28 deg.

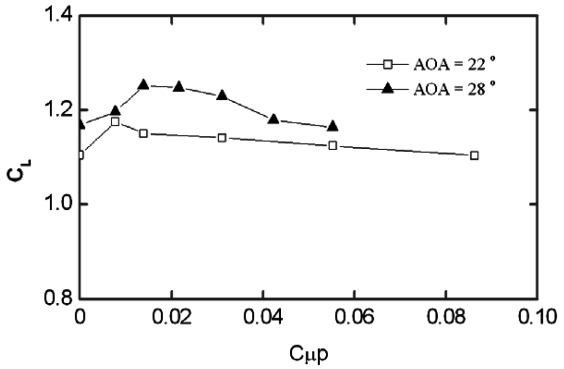

Fig. 12 Measured lift coefficient C_L with $C_{\mu P}$ for port side blowing only ($C_{\mu S} = 0$) at AOA = 22 deg and 28 deg.

vortex breakdown on the port side and promotes vortex breakdown on the starboard side, resulting in a lift differential between the two sides. It is noted that the roll moment initially decreases for small blowing momentum. Interestingly, flow visualization pictures reveal that at such low blowing momentum, the vortex breakdown at the nonblowing side was also delayed rather than promoted (compare Fig. 10b with 10a), which gives rise to the negative roll moment. It is not clear as to what contributes to this vortex breakdown delay on the nonblowing side at such low blowing momentum. The corresponding lift coefficients are presented in Fig. 12. It can be seen that for port side blowing only, increasing the blowing momentum results in an increase in the lift coefficient until a maximum value is attained, and further increase in the blowing momentum leads to a reduction in the lift coefficient. This is due to the fact that at a relative small blowing momentum condition, the favorable effect of the port side blowing is stronger resulting in a net gain in the lift coefficient, and that at a higher blowing momentum condition, the unfavorable effect of the port side blowing is stronger resulting in a net loss in the lift coefficient (see Figs. 9b, 9c, 10b, and 10c).

C. Further Discussion on a Single Side/Differential Forebody Slot Blowing

From the flow visualization results of differential blowing, it can be observed that blowing on one side delays the vortex breakdown position on that side, but promotes the vortex breakdown on the other side. In our previous study [39], we postulated that the unfavorable effect of blowing on the nonblowing side is possibly caused by side-slip effect due to blowing as the entrainment of the flow by the ejected fluid potentially creates a crossflow component from the nonblowing side. Similar observations were also reported by some earlier studies with other control techniques such as asymmetric trailing-edge blowing [23,27] or asymmetric along-the-core blowing [34]. Mitchell et al. [27] postulated that "the asymmetric blowing blocks the flow on the side where it is applied, and as a result, the flow works its way to the other side" in their asymmetric (i.e., single side) trailing-edge blowing study. Although in their asymmetry along-the-core blowing study, Mitchell et al. [34] believed that "the asymmetry flow control influences both the controlled and uncontrolled leading-edge vortices, denoting an interaction between the two leading-edge vortices." However, how these vortices interact is not well understood.

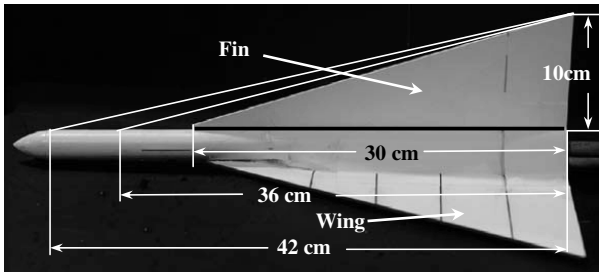

Fig. 13 Photographs of the model with a short fin of 30 cm long. [The other two longer fins (36 and 42 cm) are indicated with two lines.]

In a vortex breakdown study without flow controlled over a delta wing by Menke et al. [42], the authors believe that the interaction between the opposite leading-edge vortices is the result of a streamwise instability, resulting in an antisymmetric motion of these vortices. However, under controlled circumstances, the fact that different asymmetry-control techniques (trailing-edge blowing, along-the-core blowing, and forebody slot blowing) lead to similar observations, suggests that the interactions between the two leading-edge vortices play an important role.

To further understand this observed phenomenon in the present case of forebody slot blowing, an experiment with various fins was conducted. Three half-delta shape vertical fins with the same height of 10 cm, and different lengths of 30 cm (short fin), 36 cm (medium fin), and 42 cm (long fin) were tested (refer to Fig. 13). They were attached to the model along the centerbody using two brackets near the trailing edge so as to minimize its effects on vortex breakdown. All fins were cut from 1-mm thick aluminum sheet and secured with white adhesive paper. The aim is to systematically isolate the effects of the slot blowing and vortex interaction by compartmentalizing the port and starboard sides with the vertical fin. The fins of different lengths are used to isolate the degree of starboard and port side interactions occurring not only on the downstream of the apex of the wing but also in the vicinity upstream of the apex. A long fin will effectively isolate any interactions and crossflow.

Figure 14 presents typical flow images with/without the presence of fins at AOA = 22 deg for different blowing conditions. Without blowing (Fig. 14a), it can be seen that vortex breakdown locations are delayed slightly for all three fins, indicating the existence of the interactions between the two leading-edge vortices. With blowing (Figs. 14b and 14c), all fins influence the vortex breakdown locations to some extent. For example, for port side blowing only (Fig. 14b), it is clearly shown that the port side vortex breakdown location moves upstream and the starboard vortex breakdown location moves downstream with increasing the fin length. It is also worth noting that for a fixed blowing momentum, vortex breakdown on the blowing side without fin is delayed considerably downstream compared to a long fin configuration [see Figs. 14b (1) and (4)]. This implies that a much higher blowing momentum is needed for the long fin configuration to achieve the same delay in vortex breakdown position as in the no fin configuration. Figures 15 and 16 summarized other blowing conditions with various fins at AOA of 22 deg. It can be observed that as port side blowing momentum increases, a delay in the port side vortex breakdown position is the smallest for the long fin, and there is almost no promotion of starboard side vortex breakdown position for the long fin.

From the above observations, it can be deduced that the long fin is the most effective in preventing the unfavorable effect on the starboard side for port side blowing only. The short fin is less effective while the medium fin has an effectiveness intermediate between the long and the short fins. Similar observations are also

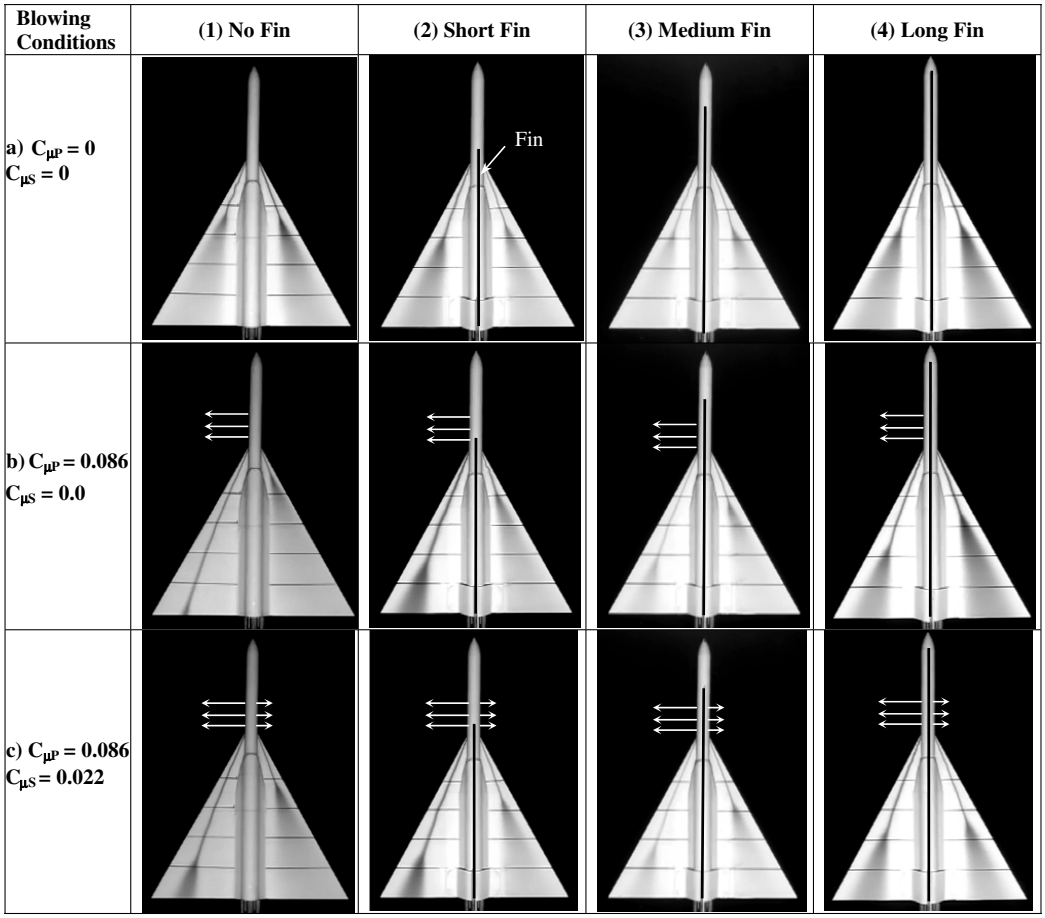

Fig. 14 Time-averaged images with and without fins at AOA = 22 deg for different blowing conditions. Note that black lines indicate the location of the fin.

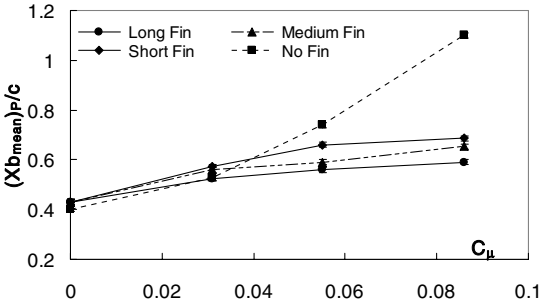

Fig. 15 Effects of fins on vortex breakdown position on port side with port side blowing only at AOA = 22 deg.

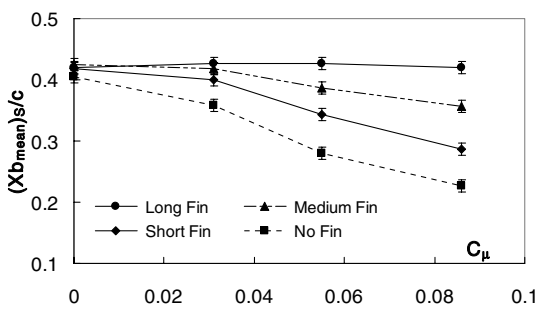

Fig. 16 Effects of fins on vortex breakdown position on starboard side with port side blowing only at AOA = 22 deg.

obtained for AOA = 17, 26, and 28 deg (results not shown here for brevity). It should be noted that all the fins have the same height with only slight differences at the front part of the fins (see Fig. 13). This implies that the flow interactions occur not only downstream of the apex of the wing but also in the vicinity upstream of the apex. A likely explanation for the interaction is that the presence of slot blowing will cause flow entrainment into this slot jet. As the jet is blown in a cross-stream direction, it will entrain fluid from the non or weaker blowing side of the forebody. A longer fin will significantly isolate this effect.

Moreover, a delay in vortex breakdown will also have a more persistent suction effect which thereafter contributes to the increased vortex lift. Further, the suction effects of one vortex may also affect the vortex on the opposite side. The net effect is that the vortex on the side of stronger blowing may cause some crossflow over the fuselage from the opposite side with little or no blowing. The end result is a further delay of vortex breakdown on the side with stronger blowing, while promoting the vortex on the opposite side. These effects are summarized as depicted in Fig. 17. The overall effect is similar to a delta wing at a side-slip angle which promotes vortex breakdown on the windward side and delays vortex breakdown on the other side. Thus, the detrimental effect of forebody slot blowing on the other side can be a combination of blowing itself and the interaction of the vortices on both sides resulting in a side-slip-like effect. The effects of differential blowing may also be explained in terms of swirl number of wing vortices. On the blowing side, the ejected fluid has a velocity component which is opposite to the swirl velocity of the vortex forming on the blowing side. This causes the swirl velocity or swirl number of the wing vortex to decrease, and thus stabilizing the vortex. In contrast, blowing induces some crossflow from the nonblowing (or weaker blowing) side, and this increases the swirl velocity or swirl number of the wing vortex on the nonblowing or (weaker blowing) side and hence promoting vortex breakdown.

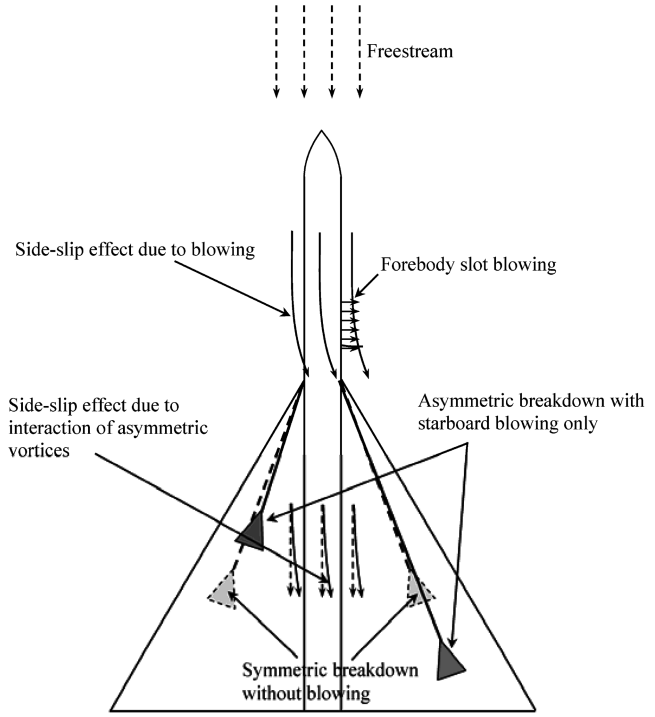

Fig. 17 Sketch of effects of a single side blowing on the flowfield.

IV. Conclusions

Flow visualization and force measurement were conducted in a water tunnel to examine the effects of forebody slot blowing on vortex breakdown and load over a generic delta wing-body configuration for the Reynolds number 8.5×10^4, and the angles of attack of 17–30 deg. Time-averaged flow images show that this technique leads to a significant delay in the formation of vortex breakdown. Correspondingly, the force measurements verify that delaying vortex breakdown increases the lift coefficient, while promoting vortex breakdown causes a reduction in lift coefficient. Symmetrical forebody slot blowing on the other hand, apart from producing a significant delay in the formation of vortex breakdown, increases the lift by more than 5%.

Both visualization studies and load measurements show that differential forebody slot blowing can be used to manipulate the vortex breakdown position and change the roll moment of the wing, which suggests that the method can be a potential means for roll control. Although blowing only on one side delays vortex breakdown, it has an opposite effect on the nonblowing side. This is analogous to a side-slip effect, like a delta wing at a certain side-slip angle leading to the occurrence of highly asymmetric vortices.

To systematically examine this possible explanation, the port and starboard sides of the model are compartmentalized with a vertical fin. The degree of starboard and port side flow interactions in the vicinity upstream of the blowing slot location and the delta wing apex can be controlled by using fins of three different lengths. The results obtained using the three fins suggest that flow entrainment by the slot jet causes a crossflow component, and this crossflow component is further enhanced by the vortex induced suction of the more persistent vortex (before vortex breakdown) over the delta wing on the side where the blowing is stronger. Therefore, the asymmetric vortex breakdown can be traced to a combination of this forebody slot blowing itself and the interaction of the vortices from both sides resulting in a side-slip-like effect.

Acknowledgments

The authors gratefully acknowledge the support from the Directorate of Research and Development, Defense Science and Technology Agency, Singapore, under the Flow Control Program POD-0103935. The authors also wish to acknowledge Huang Weiquan for his assistance with the experiments and to thank the reviewers for their valuable comments and suggestions on the manuscript.

References

[1] Peckham, D. H., and Atkinson,S. A., "Preliminary Results of Low Speed Wind Tunnel Tests on a Gothic Wing of Aspect Ratio 1.0," *British Aeronautical Research Council* CP 508, Her Majesty's Stationery Office, London, April 1957, pp. 1–37.

[2] Hall, M. G., "Vortex Breakdown," *Annual Review of Fluid Mechanics*, Vol. 4, Jan. 1972, pp. 195–218. doi:10.1146/annurev.fl.04.010172.001211

[3] Leibovich, S., "The Structure of Vortex Breakdown," *Annual Review of Fluid Mechanics*, Vol. 10, Jan. 1978, pp. 221–246. doi:10.1146/annurev.fl.10.010178.001253

[4] Escudier, M. P., "Vortex Breakdown: Observations and Explanations," *Progress in Aerospace Sciences*, Vol. 25, No. 2, 1988, pp. 189–229. doi:10.1016/0376-0421(88)90007-3

[5] Délery, J. M., "Aspects of Vortex Breakdown," *Progress in Aerospace Sciences*, Vol. 30, No. 1, 1994, pp. 1–59. doi:10.1016/0376-0421(94)90002-7

[6] Althaus, W., Brucker, C., and Weimer, M., "Breakdown of Slender Vortices," *Fluid Vortices*, edited by S. Green, Kluwer Academic, Norwell, MA, 1995, pp. 373–426.

[7] Lucca-Negro, O., and O'Doherty, T., "Vortex Breakdown: A Review," *Progress in Energy and Combustion Science*, Vol. 27, No. 4, 2001, pp. 431–481. doi:10.1016/S0360-1285(00)00022-8.

[8] Mitchell, A. M., and Délery, J., "Research into Vortex Breakdown Control," *Progress in Aerospace Sciences*, Vol. 37, No. 4, May 2001, pp. 385–418. doi:10.1016/S0376-0421(01)00010-0

[9] Rao, D. M., "Leading-Edge Vortex Flap Experiments on a 74° Delta Wing," NASA CR 159161, 1979.

[10] Karagounis, T., Maxworthy, T., and Spedding, G. R., "Generation and Control of Separated Vortices Over a Delta Wing by Means of Leading-Edge Flaps," AIAA Paper 89-0997, March 1989.

[11] Gursul, I., Yang, H., and Deng, Q., "Control of Vortex Breakdown with Leading-Edge Devices," AIAA Paper 94-1857, June 1994.

[12] Gursul, I., Srinivas, S., and Batta, G., "Active Control of Vortex Breakdown Over a Delta Wing," *AIAA Journal*, Vol. 33, No. 9, 1995, pp. 1743–1745.

[13] Wahls, R. A., Vess, R. J., and Moskovitz, C. A., "Experimental Investigation of Apex Fence Flaps on Delta Wings," *Journal of Aircraft*, Vol. 23, No. 10, 1986, pp. 789–797.

[14] Behrbohm, H., "Basic Low-Speed Aerodynamics of the Short-Coupled Canard Configuration of Small Aspect Ratio," SAAB TN-60, Sweden, July 1965.

[15] Lamar, J. E., "Analysis and Design of Strake-Wing Configurations," *Journal of Aircraft*, Vol. 17, No. 1, 1980, pp. 20–27.

[16] Er-El, J., and Seginer, A., "Vortex Trajectories and Breakdown on Wing-Canard Configurations," *Journal of Aircraft*, Vol. 22, No. 8, 1985, pp. 641–648.

[17] Er-El, J., "Effect of Wing/Canard Interference on the Loading of a Delta Wing," *Journal of Aircraft*, Vol. 25, No. 1, 1988, pp. 18–24.

[18] Tu, E. L., "Navier-Stokes Simulation of a Close-Coupled Canard-Wing-Body Configuration," *Journal of Aircraft*, Vol. 29, No. 5, 1992, pp. 830–838.

[19] Tu, E. L., "Effect of Canard Deflection on Close-Coupled Canard-Wing-Body Aerodynamics," *Journal of Aircraft*, Vol. 31, No. 1, 1994, pp. 138–145.

[20] Tu, E. L., "Vortex-Wing Interaction of a Close-Coupled Canard Configuration," *Journal of Aircraft*, Vol. 31, No. 2, 1994, pp. 314–321.

[21] Hummel, D., and Oelker, H. C., "Low-Speed Characteristics for the Wing-Canard Configuration of the International Vortex Flow Experiment," *Journal of Aircraft*, Vol. 31, No. 4, 1994, pp. 868–878.

[22] Howard, R. M., and O'Leary, J. F., "Flowfield Study of a Close-Coupled Canard Configuration," *Journal of Aircraft*, Vol. 31, No. 4, 1994, pp. 908–914.

[23] Helin, H., and Watry, C. W., "Effects of Trailing-Edge Jet Entrainment on Delta Wing Vortices," *AIAA Journal*, Vol. 32, No. 4, 1994, pp. 802–804.

[24] Nawrocki, D., "Differential and Vectored Trailing-Edge Jet Control of Delta Wing Vortices," AIAA Paper 95-0008, Jan. 1995.

[25] Shih, C., and Ding, Z., "Trailing-Edge Jet Control of Leading Edge Vortices of a Delta Wing," *AIAA Journal*, Vol. 34, No. 7, 1996, pp. 1447–1456.

[26] Vorobieff, P. V., and Rockwell, D. O., "Vortex Breakdown on Pitching Delta Wing: Control by Intermittent Trailing-Edge," *AIAA Journal*, Vol. 36, No. 4, 1998, pp. 585–589.
[27] Mitchell, A. M., Molton, P., Barberis, D., and Délery, J., "Control of Leading-Edge Vortex Breakdown by Trailing-Edge Injection," *Journal of Aircraft*, Vol. 39, No. 2, 2002, pp. 221–226.
[28] Wang, J. J., Li, Q. S., and Liu, J. Y., "Effects of a Vectored Trailing Edge Jet on Delta Wing Vortex Breakdown," *Experiments in Fluids*, Vol. 34, No. 5, 2003, pp. 651–654. doi:10.1007/s00348-003-0615-z
[29] Parmenter, K., and Rockwell, D., "Transient Response of Leading-Edge Vortices to Localized Suction," *AIAA Journal*, Vol. 28, No. 6, 1990, pp. 1131–1132.
[30] Miller, S., and Gile, B., "The Effects of Blowing on Delta Wing Vortices During Dynamic Pitching at High Angles of Attack," AIAA Paper 92-0407, Jan. 1992.
[31] Kuo, C. H., and Lin, D. C., "Non-Uniform Recovery of Vortex Breakdown Over Delta Wing in Response to Blowing Along Vortex Core," *Experiments in Fluids*, Vol. 22, No. 1, 1996, pp. 33–44. doi:10.1007/BF01893304
[32] Kuo, C. H., Lu, N. Y., and Lin, D. C., "Evolution of Vertical Structure Over Delta Wing with Transient Along-Core Blowing," *AIAA Journal*, Vol. 35, No. 4, 1997, pp. 617–624.
[33] Kuo, C. H., and Lu, N. Y., "Unsteady Vortex Structure Over Delta-Wing Subject to Transient Along-Core Blowing," *AIAA Journal*, Vol. 36, No. 9, 1998, pp. 1658–1664.
[34] Mitchell, A. M., Barberis, D., Molton, P., and Délery, J., "Oscillation of Vortex Breakdown Location and Blowing Control of the Time Averaged Location," *AIAA Journal*, Vol. 38, No. 5, 2000, pp. 793–803.
[35] Dixon, C. J., "Lift Augmentation by Lateral Blowing Over a Lifting Surface," AIAA Paper 69-193, Feb. 1969.
[36] Seginer, A., and Salomon, M., "Augmentation of Fighter Aircraft Performance by Spanwise Blowing Over the Wing Leading Edge," NASA TM-84330, March 1983.
[37] Rao, D. M., "Recent Studies of Slot-Blowing Techniques for Vortex Breakdown Control on Slender Configurations," *Fluid Dynamics of High Angle of Attack, IUTAM Symposium Tokyo/Japan, Session T.3: Flow Control*, Springer–Verlag, Berlin, 1992, pp. 237–253.
[38] Bradley, R. G., and Wray, W. O., "A Conceptual Study of Leading-Edge Vortex Enhancement by Blowing," *Journal of Aircraft*, Vol. 11, No. 1, 1974, pp. 33–38.
[39] Cui, Y. D., Lim, T. T., and Tsai H. M., "Control of Vortex Breakdown Over a Delta Wing Using Forebody Slot Blowing," *AIAA Journal*, Vol. 45, No. 1, 2007, pp. 110–117. doi:10.2514/1.22575
[40] Gatlin, G. M., and McGrath, B. E., "Low-Speed Longitudinal Aerodynamic Characteristics Through Poststall for Twenty-One Novel Planform Shapes," NASA TP 3503, Aug. 1995.
[41] Munro, C., Jouannet, C., and Krus, P., "Flow Visualization and Force and Moment Correlations in a Water Tunnel," *7th Triennial International Symposium on Fluid Control, Measurement and Visualization*, Nil, Sorrento, Italy, 25–28 Aug. 2003.
[42] Menke, M., Yang, H., and Gursul, I., "Experiments on the Unsteady Nature of Vortex Breakdown Over Delta Wings," *Experiments in Fluids*, Vol. 27, No. 3, 1999, pp. 262–272. doi:10.1007/s003480050351

F. Coton
Associate Editor